

## Time-Resolved Resonance Raman Investigation of the 2-Fluorenylnitrenium Ion Reactions with C8 Guanosine Derivatives

Jiadan Xue, Pik Ying Chan, Yong Du, Zhen Guo, Cecilia Wan Ying Chung, Patrick H. Toy, and David Lee Phillips\*

Department of Chemistry, The University of Hong Kong, Pokfulam Road, Hong Kong, P. R. China

Received: June 20, 2007; In Final Form: September 8, 2007

A nanosecond time-resolved resonance Raman (ns-TR<sup>3</sup>) spectroscopic study of the reactions of the 2-fluorenylnitrenium ion with several C8-substituted guanosine derivatives is reported. The TR<sup>3</sup> spectra show that the 2-fluorenylnitrenium ion reacts with the C8-substituted guanosine derivatives (C8-methylguanosine and C8-bromoguanosine) to produce C8 intermediates with the methyl and bromine moieties still attached to the intermediate species at the C8 position. The C8-bromoguanosine species was observed to be less reactive toward the 2-fluorenylnitrenium ion compared to the guanosine and C8-methylguanosine species. Comparison of the TR<sup>3</sup> spectra to the results obtained from density functional theory calculations was used to characterize the C8 intermediates observed to learn more about their structure and properties. The implications of these results for the chemical reactivity of arylnitrenium ions toward substituted guanosine derivatives are briefly discussed.

### Introduction

Because arylnitrenium ions are thought to be key reaction intermediates in the chemical carcinogenesis of aromatic amines, there has been a great deal of interest in studying their properties and reactions.<sup>1–18</sup> Some arylnitrenium ions have been found to be selectively trapped by guanine bases in DNA, and in many cases these reactions produce noticeable amounts of C8 adducts.<sup>8–10,14,18</sup> Arylnitrenium ions are typically very reactive and short-lived species which are difficult to investigate in room-temperature solutions. To better study the properties and reactions of arylnitrenium ions, several groups have developed photochemical methods to generate arylnitrenium ions so that time-resolved spectroscopic techniques can be used to study them.<sup>19–33</sup> One of the photochemical methods developed to produce arylnitrenium ions employs the photolysis of aryl azides to generate a singlet arylnitrene which then reacts very quickly with water to form a singlet arylnitrenium ion.<sup>19–29</sup> Picosecond transient absorption and time-resolved resonance Raman (TR<sup>3</sup>) experiments have directly observed that the 2-fluorenylnitrenium ion is generated about 100 ps after photolysis of 2-fluorenyl azide in a mixed aqueous solvent.<sup>25,34</sup>

There are not many reports of time-resolved vibrational spectroscopic studies of arylnitrenium ions and their reactions in room-temperature solutions. Time-resolved infrared (TRIR)<sup>30</sup> has been used to study several arylnitrenium ions in some organic solvents.<sup>30,35</sup> We have recently demonstrated the utility of using time-resolved resonance Raman (TR<sup>3</sup>) spectroscopy to study a range of arylnitrenium ions in mixed aqueous solvents.<sup>36,38</sup> Recently we have reported the first time-resolved vibrational spectroscopic observation of an arylnitrenium ion reaction with a guanine derivative to make a C8 intermediate.<sup>38</sup> This study also provided the first time-resolved vibrational characterization of the structure and properties of a C8 intermediate.<sup>38</sup> In this paper, we report a TR<sup>3</sup> study of the

reactions of the 2-fluorenylnitrenium ion with several C8-substituted guanosine derivatives. We observed intermediates formed from the reactions of the 2-fluorenylnitrenium ion with C8-bromoguanosine and C8-methylguanosine and compare the results obtained for the vibrational spectra, structure, and properties to those previously reported for the analogous reaction with guanosine.<sup>38</sup> The bromine atom substitution at the C8 position was found to moderately influence the 2-fluorenylnitrenium ion reaction with C8-bromoguanosine compared to the reactions with guanosine and C8-methylguanosine. Substituent effects at the C8 position on the reactions of the 2-fluorenylnitrenium ion with substituted guanosines and their relevant C8 intermediates are discussed. The structure, properties, and chemical reactivity of the substituted C8-intermediates are also discussed.

### Experimental and Computational Methods

The samples of C8-bromoguanosine and guanosine were purchased from Aldrich and used as is in the TR<sup>3</sup> experiments. The preparation of the 2-fluorenyl azide precursor for the 2-fluorenylnitrenium ion was done by following literature methods<sup>40</sup> and is detailed in the Supporting Information. The C8-methylguanosine sample was prepared following literature methods<sup>39,41</sup> and is also detailed in the Supporting Information. Spectroscopic grade acetonitrile and deionized water were used in preparing samples in conjunction with a 0.002 M Na<sub>2</sub>HPO<sub>4</sub>–0.002 M NaH<sub>2</sub>PO<sub>4</sub> buffer. Samples of 0.3 mM 2-fluorenyl azide and 0.9 mM C8-bromoguanosine or C8-methylguanosine or guanosine were prepared in a water–acetonitrile (50:50 by volume) solvent with a 0.002 M Na<sub>2</sub>HPO<sub>4</sub>–0.002 M NaH<sub>2</sub>PO<sub>4</sub> buffer for use in the TR<sup>3</sup> experiments.

The experimental apparatus and methods used to obtain the nanosecond time-resolved resonance Raman (ns-TR<sup>3</sup>) experiments<sup>37,38</sup> have been detailed previously so only a short description will be presented here. The hydrogen Raman shifted laser lines for the harmonics of a Nd:YAG nanosecond pulsed laser system

\* To whom correspondence should be addressed. Phone: 852-2859-2160. Fax: 852-2857-1586. E-mail: phillips@hkucc.hku.hk.

produced the 309.1 nm pump (first anti-Stokes Raman shifted line of the 355 nm third harmonic) and 368.9 nm probe (second anti-Stokes Raman shifted line of the 532 nm second harmonic) wavelengths employed in the ns-TR<sup>3</sup> experiments. The ns-TR<sup>3</sup> experiments utilized two Nd:YAG lasers electronically synchronized to each other by a pulse delay generator used to control the relative timing of the two lasers that was monitored using a fast photodiode and a 500 MHz oscilloscope. The jitter between the pump and probe laser pulses was observed to be <5 ns, and the laser beams were lightly focused onto a flowing liquid stream of sample using a near collinear backscattering geometry. The Raman scattered light was collected using a backscattering geometry and reflective optics that imaged the light through a depolarizer and entrance slit of a 0.5 m spectrograph that dispersed the light onto a liquid-nitrogen-cooled CCD detector. The Raman signal was accumulated for about 30–60 s before being read out to an interfaced PC computer, and about 10–20 of these read outs were summed to obtain the Raman spectrum. The TR<sup>3</sup> spectra were determined by subtracting the pump–probe spectrum at negative 100 ns from the pump–probe spectra acquired at positive delay times so as to remove the solvent and precursor Raman bands. The known wavenumbers of the mixed solvent acetonitrile Raman bands were employed to calibrate the wavenumber of the TR<sup>3</sup> spectra to an absolute accuracy of about  $\pm 3$  cm<sup>-1</sup> (and a relative accuracy of  $\pm 1$ –2 cm<sup>-1</sup> from scan to scan), and a Lorentzian function was utilized to integrate the relevant Raman bands to find their areas and determine the decay and growth kinetics of the species observed in the TR<sup>3</sup> experiments.

All of the density functional theory calculated reported here made use of the Gaussian program suite.<sup>42</sup> The complete geometry optimization and vibrational frequency computations were done analytically using the BPW91 method with the cc-PVDZ basis set for the species of interest. A Lorentzian function with a 20 cm<sup>-1</sup> bandwidth was used in conjunction with the calculated Raman vibrational frequencies and relative intensities to find the calculated BPW91/cc-PVDZ Raman spectra presented here.

## Results and Discussion

**A. Time-Resolved Resonance Raman (TR<sup>3</sup>) Spectroscopy of the 2-Fluorenylnitrenium Ion Reactions with Guanosine, C8-Methylguanosine, and C8-Bromoguanosine.** Figures 1–3 display the selected ns-TR<sup>3</sup> spectra acquired at varying time delays after photolysis of 0.3 mM 2-fluorenyl azide in water–acetonitrile (50:50 by volume) solvent with a 0.002 M Na<sub>2</sub>HPO<sub>4</sub>–0.002 M NaH<sub>2</sub>PO<sub>4</sub> buffer that contain 0.9 mM guanosine (Figure 1), 0.9 mM C8-methylguanosine (Figure 2), and 0.9 mM C8-bromoguanosine (Figure 3). The overview of ns-TR<sup>3</sup> spectra with more time delays and wider wavenumber ranges are displayed as Figures 1S–3S in the Supporting Information. The time delays between the pump (309.1 nm) and probe (368.9 nm) laser pulses are shown to the right of each spectrum, and the Raman shifts of selected bands are presented above the Raman bands of several spectra. The TR<sup>3</sup> spectra displayed in Figures 1–3 are all almost the same at early time delays (see the 10 ns spectra in the figures), and this indicates that the same species is observed at early times. This first species can be readily assigned to the 2-fluorenylnitrenium ion that we have observed after photolysis of 2-fluorenyl azide in aqueous environments in previous work.<sup>36,37d,38</sup> The 10 ns spectra shown in Figures 1–3 are compared to the TR<sup>3</sup> spectrum of the 2-fluorenylnitrenium ion reported in ref 36a in Figure 4S of the Supporting Information. This comparison confirms the first

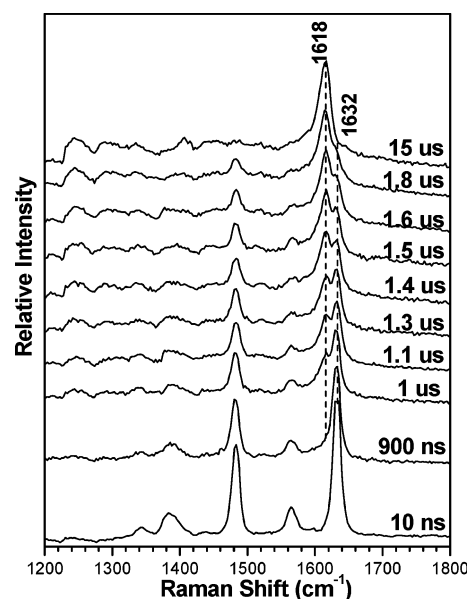


**Figure 1.** Selected TR<sup>3</sup> spectra obtained by 368.9 nm probe after 309.1 nm photolysis of 0.3 mM 2-fluorenyl azide in the presence of 0.9 mM guanosine in a water–acetonitrile (50:50) mixed solvent with a 0.002 M Na<sub>2</sub>HPO<sub>4</sub>–0.002 M NaH<sub>2</sub>PO<sub>4</sub> buffer. The time delays between the pump (309.1 nm) and probe (368.9 nm) laser beams are shown to the right of each spectrum, and the Raman shifts of selected bands are presented at the top of the 15  $\mu$ s spectrum. An overview of the TR<sup>3</sup> spectra with more time delays and wider wavenumber range is presented in Figure 1S in the Supporting Information. See text for more details.

species observed in the ns-TR<sup>3</sup> spectra of Figures 1–3 is the 2-fluorenylnitrenium ion. Inspection of the ns-TR<sup>3</sup> spectra of Figures 1–3 reveals that the Raman bands of the 2-fluorenylnitrenium ion decrease in intensity over the hundreds of nanoseconds to microseconds time scale and Raman bands due to some reaction and another species are formed. The growth in the intensity of the new species Raman bands appear to be correlated with the decay of the 2-fluorenylnitrenium ion.

The larger Raman bands in the 1600 cm<sup>-1</sup> region of the ns-TR<sup>3</sup> spectra in Figures 1–3 (the  $\sim 1630$  cm<sup>-1</sup> Raman band for the 2-fluorenylnitrenium ion, the 1618 cm<sup>-1</sup> band for the intermediate shown in Figure 1, the 1613 cm<sup>-1</sup> band for the intermediate shown in Figure 2, and the 1614 cm<sup>-1</sup> band for the intermediate shown in Figure 3) can be used to monitor the decay of the 2-fluorenylnitrenium ion and the growth of the second species. Figure 4 displays plots of the integrated intensities of the relevant Raman marker bands for the reaction of the 2-fluorenylnitrenium ion with guanosine (Figure 4A), C8-methylguanosine (Figure 4B), and C8-bromoguanosine (Figure 4C). The decay of the 2-fluorenylnitrenium ion and the growth of the new species were simultaneously fit satisfactorily (see line fits to the data of Figure 4) by common time constant exponential decay and growth functions, respectively. This and the fact that the new species are only observed in the presence of the guanosine derivatives indicate that the new species are directly formed from the reaction of the 2-fluorenylnitrenium ion with the respective guanosine derivative. The fits to the data shown in Figure 4 found time constants of about 840 ns for the reaction with guanosine, 835 ns for the reaction with C8-methylguanosine, and 1765 ns for the reaction with C8-bromoguanosine.

Our previous study showed that the 2-fluorenylnitrenium ion reacts with guanosine to directly produce a C8-intermediate species.<sup>38</sup> The ns-TR<sup>3</sup> spectra shown in Figure 1 for the reaction of the 2-fluorenylnitrenium ion with guanosine are in excellent agreement with similar spectra from our previous study of this

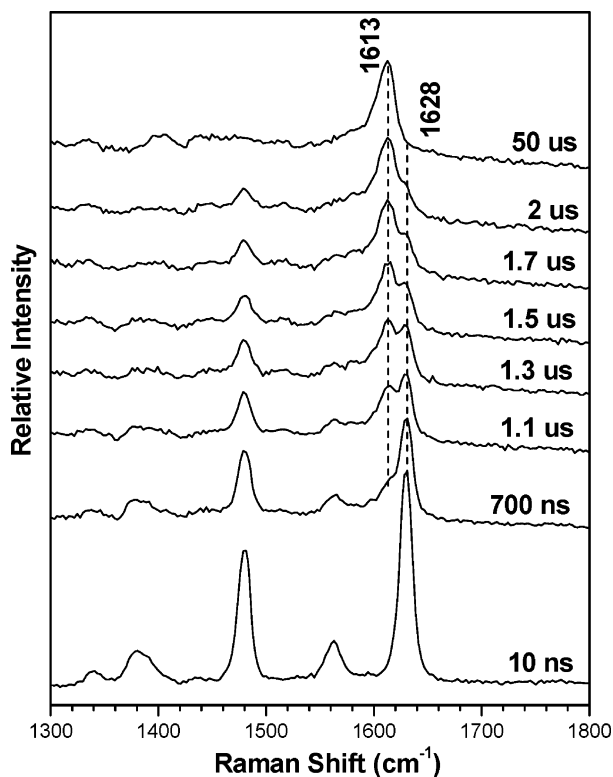


**Figure 2.** Selected TR<sup>3</sup> spectra obtained by 368.9 nm probe after 309.1 nm photolysis of 0.3 mM 2-fluorenyl azide in the presence of 0.9 mM C8-methylguanosine in a water–acetonitrile (50:50) mixed solvent with a 0.002 M Na<sub>2</sub>HPO<sub>4</sub>–0.002 M NaH<sub>2</sub>PO<sub>4</sub> buffer. The time delays between the pump (309.1 nm) and probe (368.9 nm) laser beams are shown to the right of each spectrum, and the Raman shifts of selected bands are presented at the top of the 50 μs spectrum. An overview of the TR<sup>3</sup> spectra with more time delays and wider wavenumber range is presented in Figure 2S in the Supporting Information. See text for more details.

reaction reported in ref 38 under somewhat different reaction conditions. Figure 5S in the Supporting Information displays a comparison of the 15 μs spectrum of Figure 1 with the 8 μs spectrum obtained in ref 38 for the C8 intermediate species, and these spectra are very similar and due to the same species. Thus, the second species observed in the TR<sup>3</sup> spectra of Figure 1 is due to the C8 intermediate formed from the reaction of the 2-fluorenylnitrenium ion and guanosine. Figure 5 shows a comparison of the ns-TR<sup>3</sup> spectra observed for the new species after the reaction of the 2-fluorenylnitrenium ion with guanosine (B), C8-methylguanosine (C), and C8-bromoguanosine (A).

Inspection of Figure 5 reveals that all three species have similar vibrational frequencies and relative intensities although they are not identical with one another. This similarity of the ns-TR<sup>3</sup> spectra indicates the second species observed in the reactions of the 2-fluorenylnitrenium ion with C8-methylguanosine and C8-bromoguanosine are likely the corresponding substituted C8 intermediates formed from the reaction of the 2-fluorenylnitrenium ion with these substituted guanosine derivatives. To check this hypothesis, we performed BPW91/cc-PVDZ density functional theory calculations for the C8 intermediates produced from the reactions of the 2-fluorenylnitrenium ion with guanosine, C8-methylguanosine, and C8-bromoguanosine where the nitrogen of the 2-fluorenylnitrenium ion attaches to the C8 position of the guanosine derivatives, and these species are the *N*-(guanosine-C8-yl)-2-aminofluorene cation, the *N*-(C8-methylguanosine-C8-yl)-2-aminofluorene cation, and the *N*-(C8-bromoguanosine-C8-yl)-2-aminofluorene cation species, which are referred to as the C8 intermediate,

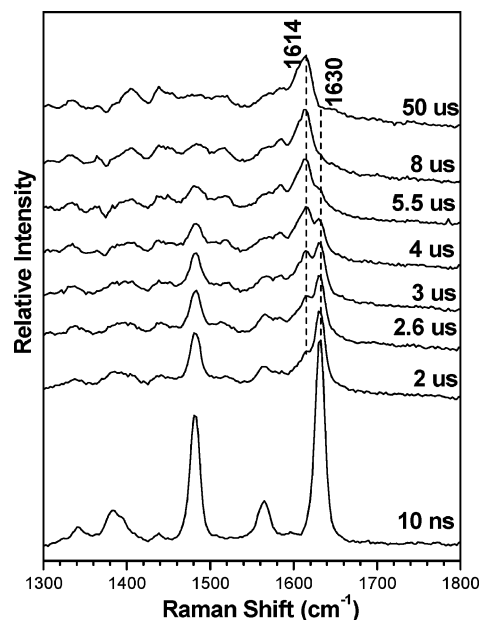


**Figure 3.** Selected TR<sup>3</sup> spectra obtained by 368.9 nm probe after 309.1 nm photolysis of 0.3 mM 2-fluorenyl azide in the presence of 0.9 mM C8-bromoguanosine in a water–acetonitrile (50:50) mixed solvent with a 0.002 M Na<sub>2</sub>HPO<sub>4</sub>–0.002 M NaH<sub>2</sub>PO<sub>4</sub> buffer. The time delays between the pump (309.1 nm) and probe (368.9 nm) laser beams are shown to the right of each spectrum, and the Raman shifts of selected bands are presented at the top of the 50 μs spectrum. An overview of the TR<sup>3</sup> spectra with more time delays and wider wavenumber range is presented in Figure 3S in the Supporting Information. See text for more details.

the C8-methyl intermediate, and the C8-bromo intermediate, respectively, hereafter. The BPW91/cc-PVDZ calculations were performed to predict the total energies, optimized geometries, and vibrational frequencies for the C8 intermediate, the C8-methyl intermediate, and the C8-bromo intermediate species. Figure 6 presents simple schematic structures of the BPW91/cc-PVDZ optimized geometries for the C8 intermediate, the C8-methyl intermediate, and the C8-bromo intermediate species with selected bond lengths (in Å) indicated next to the appropriate bonds, and Table 1S lists selected structural parameters for the optimized geometries. Figure 7 compares the ns-TR<sup>3</sup> spectra in Figures 1–3 (time delays of 15, 50, and 50 μs, respectively) for the new species observed from the reactions of the 2-fluorenylnitrenium ion with the guanosine derivatives to the BPW91/cc-PVDZ calculated normal Raman spectra (whose relative intensities were convoluted with a Lorentzian function) for the C8 intermediate, the C8-methyl intermediate, and the C8-bromo intermediate species. Tables 2S–4S compare the experimental Raman band vibrational frequencies from the ns-TR<sup>3</sup> spectra of Figure 7 to the BPW91/cc-PVDZ calculated normal Raman vibrational frequencies for the C8 intermediate, the C8-methyl intermediate, and the C8-bromo intermediate species.

Inspection of Figure 7 reveals that the experimental TR<sup>3</sup> spectra show reasonable agreement with the calculated normal Raman spectra for the C8 intermediate, the C8-methyl intermediate, and the C8-bromo intermediate species, respectively, with some moderate differences in the relative intensities that can be easily accounted for by the fact that the experimental spectra are resonantly enhanced while the calculated spectra are for normal (or nonresonant) Raman spectra. Examination of Tables 2S–4S shows there is generally good agreement between the experimental and calculated vibrational frequencies with the calculated vibrational frequencies being within about 4.5, 5.5,

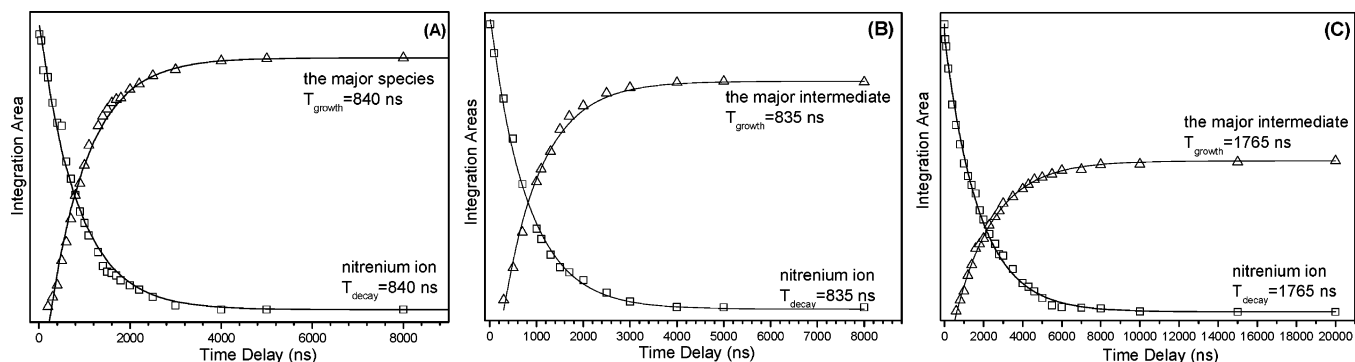


**Figure 4.** Plots of the integrated areas for the characteristic Raman bands for the species observed in the TR<sup>3</sup> spectra of Figure 1 (graph A), Figure 2 (graph B), and Figure 3 (graph C). The data for the about 1630 cm<sup>-1</sup> Raman band for the 2-fluorenylnitrenium ion are shown as open squares, and the data for the characteristic Raman band for the respective major intermediate Raman bands at about 1614 cm<sup>-1</sup> are given as open triangles as a function of time delay between the pump and probe laser pulses. The data were fit to simple exponential growth and/or decay functions as shown by the curves in the graphs. The time constants for the best fit exponential kinetics are indicated next to the appropriate curves for the 2-fluorenylnitrenium ion decay and the growth of the major intermediates.

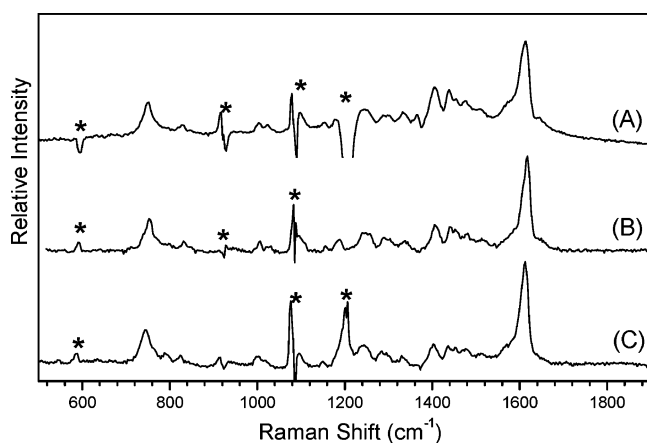


**Figure 5.** Comparison of (A) the 50 μs TR<sup>3</sup> spectrum from Figure 3 (in the presence of C8-bromoguanosine) and (C) the 50 μs TR<sup>3</sup> spectrum from Figure 2 (in the presence of C8-methylguanosine) to (B) a 8 μs TR<sup>3</sup> spectrum previously reported for the C8 intermediate in ref 38 that was obtained after photolysis of 2-fluorenyl azide in the presence of guanosine in a mixed aqueous solvent. Star symbols mark solvent-subtraction, stray-light, and ambient-light artifacts. See text for more details.

and 6 cm<sup>-1</sup> on average for the 17 experimental Raman band frequencies for the C8 intermediate, the C8-methyl intermediate, and the C8-bromo intermediate species, respectively, compared to calculated ones. These results suggest that the ns-TR<sup>3</sup> spectra in Figures 1–3 (time delays of 15, 50, and 50 μs, respectively) for the new species observed from the reactions of the 2-fluorenylnitrenium ion with the guanosine derivatives can be tentatively assigned to the C8 intermediate, the C8-methyl intermediate, and the C8-bromo intermediate species.

**B. Discussion of the Structure and Properties of the C8 Intermediate, the C8-Methyl Intermediate, and the C8-Bromo Intermediate Species.** Examination of Figure 6 reveals that there are moderate differences in the structure and properties of the C8-methyl intermediate and the C8-bromo intermediate species. These differences in the structure appear mainly in the ring 1 of the guanosine moiety, the carbon–nitrogen bonds connecting the guanosine and 2-fluorenylnitrenium ion moieties, and ring 1 of the 2-fluorenylnitrenium ion moiety of the respective intermediates. Some selected bonds lengths are presented in Table 1. For example, the C37–N34 and C8–N34 bonds connecting the guanosine and 2-fluorenylnitrenium ion moieties increase 0.0093 and 0.0317 Å, respectively, in C8-methyl intermediate compared to C8 intermediate and decrease

0.0190 and 0.0640 Å in the C8-bromo intermediate compared to C8 intermediate. These values indicate that attachment of the 2-fluorenylnitrenium ion at the C8 position of C8-methyl guanosine leads to weaker C37–N34 and C8–N34 bonds in the C8-methyl intermediate compared to the C8 intermediate produced from the analogous reaction with the guanosine substrate. In contrast, the attachment of the 2-fluorenylnitrenium ion at the C8 position of C8-bromo guanosine results in stronger C37–N34 and C8–N34 bonds in the C8-bromo intermediate compared to the C8 intermediate produced from the analogous reaction with the guanosine substrate. The qualitatively different behavior in the C8-methyl and C8-bromo substituents on the C37–N34 and C8–N34 bonds in their respective C8 intermediates can be attributed to the methyl moiety being an electron donor and the bromo moiety being an electron acceptor. The differing character of the C8-methyl and C8-bromo substitutions also results in similar qualitatively different behavior on the C8–N9 and C8–N7 bonds of ring 1 of the guanosine moiety in the intermediates. For example, the C8–N9 and C8–N7 bonds of ring 1 of the guanosine moiety in C8-methyl intermediate increase 0.0142 and 0.0066 Å compared to C8 intermediate but in the C8-bromo intermediate decrease 0.0395 and 0.0332 Å, respectively, compared to the C8 intermediate. The changes in the C37–N34, C8–N34, C8–N9, and C8–N7 bonds in the substituted C8 intermediates compared to the C8 intermediate are generally noticeably larger for the C8-bromo substitution than for the C8-methyl substitution. It is interesting to note that the N7–C5, N9–C4, and C4–C5 bonds of ring 1 of the guanosine moiety are not affected as much as the C37–N34, C8–N34, C8–N9, and C8–N7 bonds in the substituted C8 intermediates compared to the C8 intermediate, and all three intermediates have similar carbon–nitrogen double bond character for the N7–C5 and N9–C4 bonds.

The C8-methyl substitution results in only small differences in ring 1 of the 2-fluorenylnitrenium ion moiety of the C8-methyl intermediate compared to the C8 intermediate, and both of these intermediates have similar cyclohexadienyl character in ring 1 of the 2-fluorenylnitrenium ion moiety. For example, C37–C36, C36–C41, C37–C38, and C38–C39 bonds in ring 1 of the 2-fluorenylnitrenium ion moiety of the C8 intermediates have bond alternations of 0.0223 and 0.0239 Å for the C8 intermediate and 0.0213 and 0.0245 Å for C8-methyl intermediate. However, the C8-bromo substitution leads to noticeably more cyclohexadienyl character in the C37–C36, C36–C41, C37–C38, and C38–C39 bonds in ring 1 of the

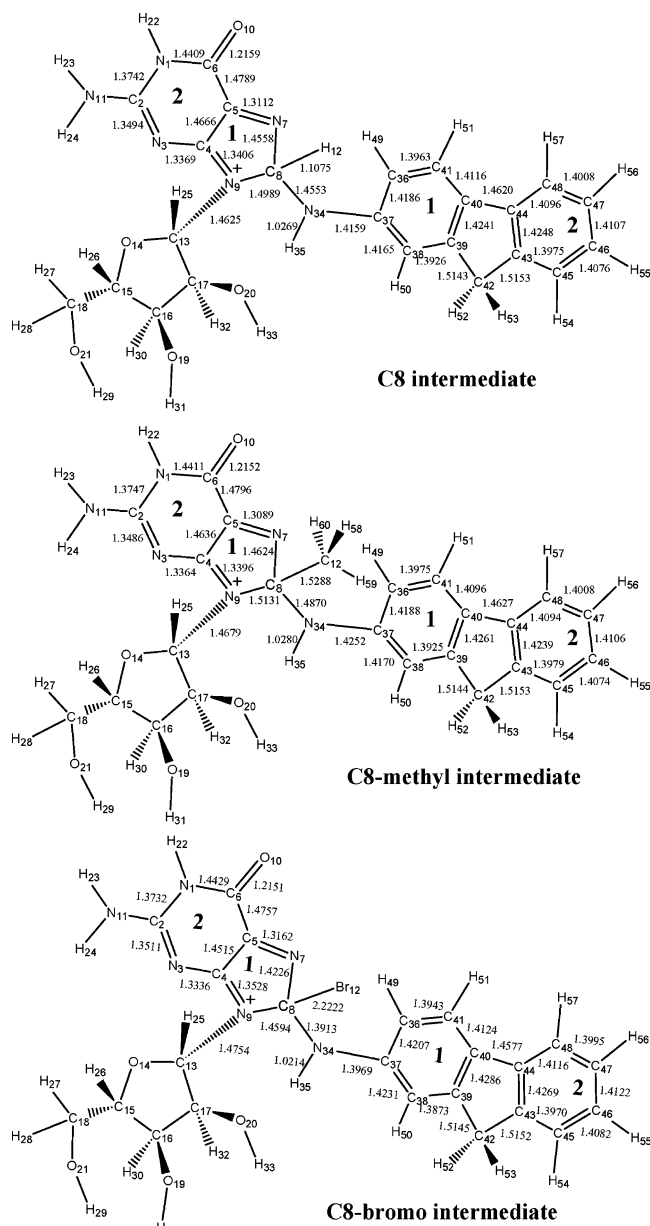


**Figure 6.** Simple schematic structures of the BPW91/cc-PVDZ optimized geometries for the C8 intermediate, the C8-methyl intermediate, and the C8-bromo intermediate species with selected bond lengths (in Å) indicated next to the appropriate bonds shown.

2-fluorenylnitrenium ion moiety for the C8-bromo intermediate where the bond alternations are 0.0264 and 0.0358 Å, respectively.

The preceding results suggest that the bromine and methyl group substitutions at the C8 position of the C8 intermediate only have modest perturbations on the overall structure and properties. This is consistent with the vibrational frequencies and experimental ns-TR<sup>3</sup> spectra of the three C8 intermediates being very similar to one another. Figure 8 shows a comparison of the ns-TR<sup>3</sup> spectra for the largest Raman bands in the 1600 cm<sup>-1</sup> region for the C8 intermediate (dashed line), the C8-methyl intermediate (dotted line), and the C8-bromo intermediate (solid line). The carbon double bond aromatic stretch modes for all of the arylnitrenium ions studied so far by TR<sup>3</sup> spectroscopy appear to be resonantly enhanced the most and are the strongest resonance Raman feature in the TR<sup>3</sup> spectra.<sup>34,36–38</sup> Both TRIR and TR<sup>3</sup> studies have shown that the vibrational frequencies of the C–C aromatic stretch vibrational band(s) correlate well with

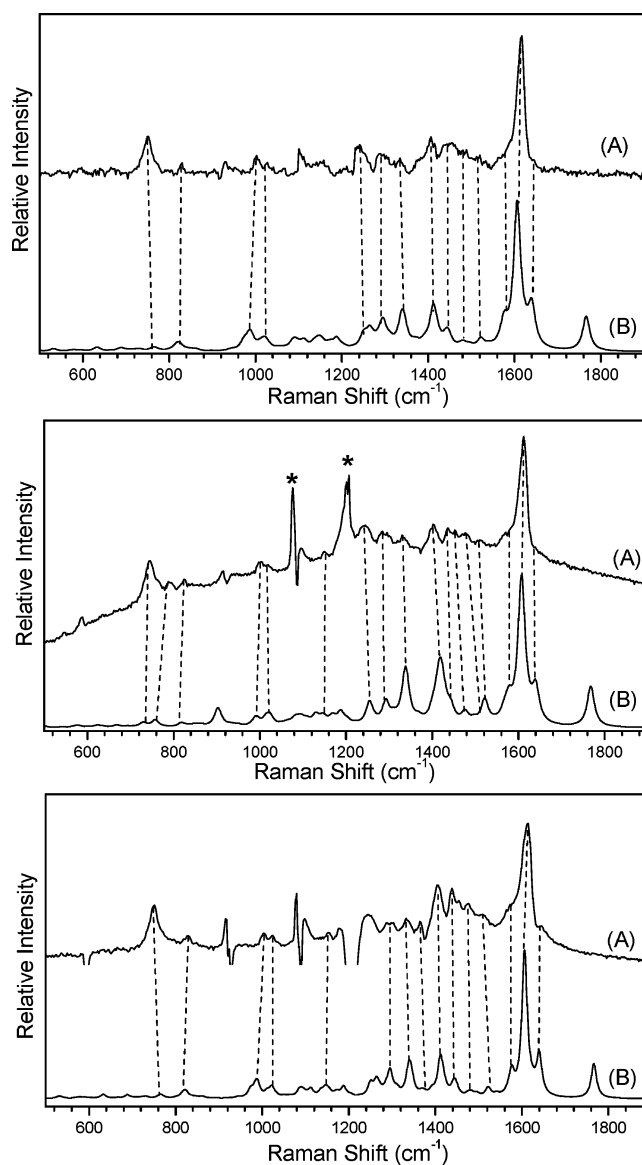


**Figure 7.** Comparison of the ns-TR<sup>3</sup> spectra (curves A) in Figures 1–3 (time delays of 15, 50, and 50 μs, respectively) for the new species observed from the reactions of the 2-fluorenylnitrenium ion with the guanosine derivatives to the BPW91/cc-PVDZ calculated normal Raman spectra (curves B, whose relative intensities were convoluted with a Lorentzian function) for the C8 intermediate (top), the C8-methyl intermediate (middle), and the C8-bromo intermediate (bottom) species. See text for more details.

the degree of imino/cyclohexadienyl character of the arylnitrenium ions.<sup>30,35,36–38</sup> We found that the strongest Raman feature in the ns-TR<sup>3</sup> spectra of the C8 intermediate is also associated with the C–C aromatic stretch vibrational band(s) and that the vibrational frequency of these Raman bands also appear to correlate reasonably well with the degree of imino/cyclohexadienyl character of the C8 intermediate species.<sup>38</sup>

Inspection of Figure 8 shows that the strong Raman features in the 1600–1630 cm<sup>-1</sup> region due mainly to the C–C aromatic stretch vibrational modes of the three C8 intermediates appear to have some noticeable differences in their band maxima and/or bandwidth. For example, the strong Raman feature for the C8-methyl intermediate (dotted line) is downshifted by about 5 cm<sup>-1</sup> to 1613 cm<sup>-1</sup> compared to the analogous band of the C8 intermediate (dashed line) that has a maximum at 1618 cm<sup>-1</sup>. This downshift in frequency occurred consistently for the ns-TR<sup>3</sup> spectra of the C8-methyl intermediate C–C aromatic stretch

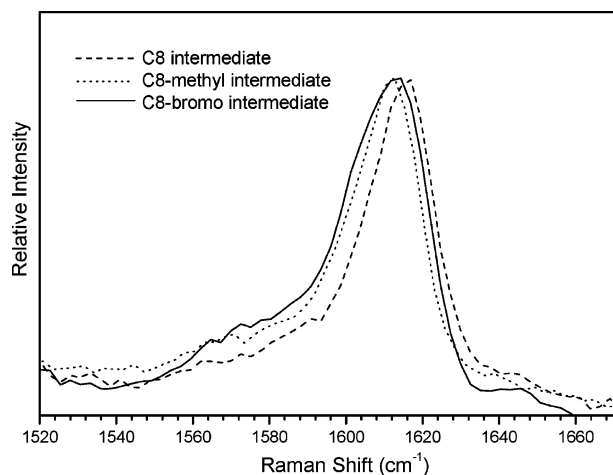


**Figure 8.** Comparison of the ns-TR<sup>3</sup> spectra around 1600 cm<sup>-1</sup> in Figures 1–3 (time delays of 50, 50, and 50  $\mu$ s, respectively) for the new species observed from the reactions of the 2-fluorenylnitrenium ion with the guanosine derivatives, the C8 intermediate (dashed line), the C8-methyl intermediate (dotted line), and the C8-bromo intermediate (solid line). See text for more details.

vibrational feature relative to that of the C8 intermediate (even when the alignment and experimental conditions were the same but the sample solutions only changed for the experiments). Examination of Tables 2S and 3S in the Supporting Information reveals that there are two modes in the 1600–1630 cm<sup>-1</sup> region mainly due to C–C aromatic stretch motions that are predicted to be at 1607 and 1610 cm<sup>-1</sup> for the C8-methyl intermediate and at 1606 and 1613 cm<sup>-1</sup> for the C8 intermediate. The predicted downshift of 3 cm<sup>-1</sup> of the  $\nu_{146}$  (C–C stretch, both ring 1 and 2 and C–N stretch of F) mode to about 1610 cm<sup>-1</sup> in the C8-methyl intermediate compared to the predicted 1613 cm<sup>-1</sup> for the  $\nu_{139}$  (C–C stretch of F, ring 1 stronger) mode for the C8 intermediate can possibly account for the experimentally observed downshift in the frequency of the strong Raman feature for the C8-methyl intermediate relative to that for the C8 intermediate insofar as the two modes in the 1600–1630 cm<sup>-1</sup> region mainly due to C=C aromatic stretch motions are both strongly resonantly enhanced in the TR<sup>3</sup> spectra for both intermediates. The downshift to 1610 cm<sup>-1</sup> in the  $\nu_{146}$  mode of the C8-methyl intermediate appears to be due to some more mixing of the C–N stretch motion in this mode combined with the C–N bonds connecting the nitrenium ion group to the C8 atom of guanosine being weaker in the C8-methyl intermediate compared to the analogous C–N bonds in the C8 intermediate. The C–C aromatic stretch Raman feature for the C8-bromo intermediate also shifts down in frequency (by about 4 cm<sup>-1</sup>) relative to the C8 intermediate feature in the ns-TR<sup>3</sup> spectra. In addition, the C–C aromatic stretch modes Raman feature for the C8-bromo intermediate becomes noticeably broader (by about 5 cm<sup>-1</sup> more bandwidth) than either the analogous Raman features for the C8 intermediate and the C8-methyl intermediate (see comparison in Figure 8). Examination of Tables 2S–4S shows that the DFT calculations predict there are three C–C aromatic stretch vibrational modes at 1604, 1615, and 1621 cm<sup>-1</sup> in the 1600–1630 cm<sup>-1</sup> region for the C8-bromo intermediate while there are only two analogous vibrational modes for the

C8 intermediate at 1606 and 1613 cm<sup>-1</sup> and for the C8-methyl intermediate at 1607 and 1610 cm<sup>-1</sup>. Therefore, the three C–C aromatic stretch vibrational modes in the C8-bromo intermediate span a range of about 17 cm<sup>-1</sup> while they only span a range of 7 and 3 cm<sup>-1</sup> respectively in the C8 intermediate and C8-methyl intermediate spectra. This suggests that resonance enhancement of the C–C aromatic stretch vibrational modes in the C8-bromo intermediate TR<sup>3</sup> spectra would lead to a noticeably broader Raman feature than for the analogous Raman feature in the C8 intermediate and C8-methyl intermediate TR<sup>3</sup> spectra, and this is consistent with the experimental observations here (see Figure 8). The DFT calculations indicate that substitution of a methyl group or a bromine atom at the C8 site of guanosine in the C8 intermediates appears to lead to noticeable perturbation of the character of the C–C stretch aromatic stretch vibrational modes with more C–N stretch motions becoming mixed with the C–C stretch motions (see basic description of the C–C aromatic stretch modes in the 1600–1630 cm<sup>-1</sup> region in Tables 2S–4S for the C8 intermediates). This appears to lead to a modest amount of downshift in the frequency of this Raman feature in the TR<sup>3</sup> spectra of the C8-methyl intermediate and the C8-bromo intermediate relative to the C8 intermediate as well as to noticeable additional broadening of this Raman feature in the C8-bromo intermediate TR<sup>3</sup> spectra.

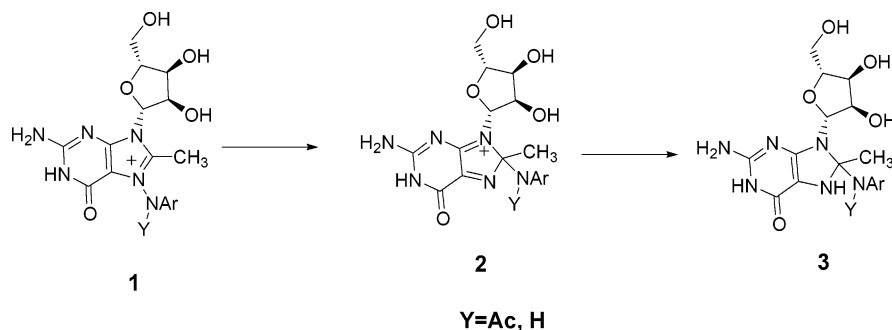
**C. Discussion of the 2-Fluorenylnitrenium Ion Reactions with Guanosine, C8-Methylguanosine, and C8-Bromoguanosine.** The major products typically produced from the reactions of arylnitrenium ions with guanine derivatives are believed to be C8 adducts like those reported from *in vivo* and *in vitro* studies.<sup>43,44</sup> But the C8 position is not regarded as the normal position for electrophilic addition in guanine, so the detailed mechanism(s) for the reactions of arylnitrenium ions with guanine derivatives are of great interest. C8-substituted guanine derivatives have been used as effective reactants to study the reaction mechanism by several groups. For example, Novak and co-workers employed C8-methylguanosine and the N-acetyl and the parent 4-biphenylnitrenium ions to study the reaction of these arylnitrenium ions with the C8-methylguanosine substrate.<sup>39</sup> Using characterization of the products by HPLC and NMR, two intermediates were observed to form rapidly and then to subsequently decompose slowly to a stable C8 adduct **3** (see Scheme 1 adapted from ref 39). Since the HPLC and NMR data showed that there are two intermediates leading to the final adduct, these two intermediates were believed to be a pair of diastereomers of the C8 intermediate **2**. These experimental results clearly demonstrated that deprotonation of the H atom at the C8 position is not necessary for the formation of the C8 adducts. Considering the basicity of the N7 position, Novak and co-workers proposed N7 as the position of initial attachment in guanine and proposed a reaction mechanism, as shown in Scheme 1.<sup>39</sup>

C8-methylguanosine has also been used by Humphreys and co-workers<sup>10</sup> in some mechanistic studies. However, it was difficult to directly determine whether the product had a N7 or C8 structure only from the mass spectra, because the N7 reduction product and the C8 product have the same molecule formula. However, bands of *m/z* 477 and 479 in the mass spectra demonstrated that the CH<sub>3</sub> group is still attached to the final

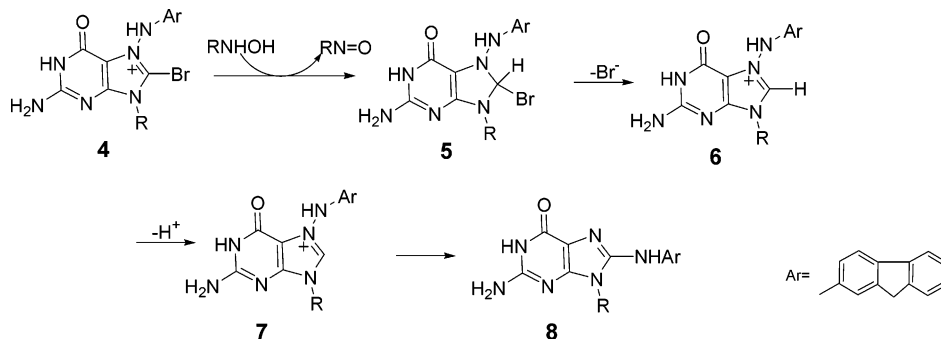
**TABLE 1: Selected Bonds Lengths (in Å) for the BPW91/cc-PVDZ Optimized Geometries for the C8 Intermediate, the C8-Methyl Intermediate, and the C8-Bromo Intermediate**

compd	C37–N34	C8–N34	C8–N9	C8–N7	C37–C36	C36–C41	C37–C38	C38–C39
C8-bromo intermediate	1.3969	1.3913	1.4594	1.4226	1.4207	1.3943	1.4231	1.3873
C8 intermediate	1.4159	1.4553	1.4989	1.4558	1.4186	1.3963	1.4165	1.3926
C8-methyl intermediate	1.4252	1.4870	1.5131	1.4624	1.4188	1.3975	1.4170	1.3925

## SCHEME 1



## SCHEME 2



product, and this is consistent with the results of Novak and co-workers<sup>39</sup> that the deprotonation of the H atom at the C8 position is not necessary for the formation of the C8 adducts to take place. Humphreys and co-workers<sup>10</sup> also examined similar reactions for C8-bromoguanosine. The major product produced from the reaction of C8-bromoguanosine and the aryl nitrenium ion used in this study had a UV spectrum identical with that of the authentic C8 adduct **8** isolated from a similar reaction with guanosine.<sup>10</sup> The  $[M + H]^+$  band at  $m/z$  463.2 in the mass spectrum indicated that the bromine atom is not attached to the product molecule. It was also noted that the yield of the C8 adduct was only about 4% and this was attributed to the small solubility of C8-bromoguanosine. They proposed a reaction mechanism as shown in Scheme 2.<sup>10</sup>

Photolysis of 2-fluorenyl azide in the presence of C8-methylguanosine and C8-bromoguanosine in aqueous environments resulted in fast formation of a 2-fluorenylnitrenium ion that subsequently reacted with the C8-substituted guanosine molecules to produce new intermediates that were observed in our TR<sup>3</sup> experiments. These intermediates were assigned to the C8-methyl intermediate and C8-bromo intermediate species respectively from comparison to a C8 intermediate spectrum formed from a similar reaction with guanosine and DFT-calculated normal Raman spectra for all of the respective C8 intermediate species as detailed in the previous section. Transient absorption quenching experiments determined that the 2-fluorenylnitrenium ion reacts with the azide anion ( $N_3^-$ ) and water with rate constants of about  $5 \times 10^9 \text{ M}^{-1} \text{ s}^{-1}$  and  $3 \times 10^4 \text{ s}^{-1}$ , respectively.<sup>32</sup> In addition, time-resolved transient absorption<sup>31</sup> and TR<sup>3</sup> experiments<sup>38</sup> indicated that the 2-fluorenylnitrenium ion reacts with guanosine with a rate constant of about  $7.6 \times 10^8 \text{ M}^{-1} \text{ s}^{-1}$ . Our previous work indicates that 2-fluorenylnitrenium ion also can be quenched by the remaining unphotolyzed precursor 2-fluorenyl azide with a rate constant of about  $3 \times 10^8 \text{ M}^{-1} \text{ s}^{-1}$ .<sup>37d</sup> Thus, guanosine or other guanine derivatives can compete with quenching of the 2-fluorenylnitrenium ion by the parent 2-fluorenyl azide species when the guanosine or other guanine derivatives have concentrations similar to or

greater than the concentration of the unphotolyzed 2-fluorenyl azide. This is consistent with our observation that, in the presence of guanosine, C8-methylguanosine, and C8-bromoguanosine, the 2-fluorenylnitrenium ion decays to produce new species assigned to the C8 intermediate, C8-methyl intermediate, and C8-bromo intermediate species. At present, it is beyond the capability of our apparatus to observe the decay of the C8 intermediates, which are still stable on the several hundreds of microseconds time scale.

The C8-bromo intermediate is formed with a time constant of about 1765 ns, and this is somewhat slower than 840 and 835 ns time constants for formation of the C8 intermediate and the C8-methyl intermediate from the similar reactions with guanosine and C8-methylguanosine, respectively (see Figure 4), under the same reaction conditions. This indicates the 2-fluorenylnitrenium ion is probably somewhat less reactive toward C8-bromoguanosine than toward guanosine or C8-methylguanosine. Table 5S of the Supporting Information presents selected structural parameters determined for guanosine, C8-methylguanosine, and C8-bromoguanosine from BPW91/cc-PVDZ calculations, and Figure 6S presents schematic diagrams for the structures of these species and the 2-fluorenylnitrenium ion. It is not exactly clear what property causes the chemical reactivity for the 2-fluorenylnitrenium ion to be less toward C8-bromoguanosine and somewhat more reactive toward guanosine and C8-methylguanosine. Inspection of Table 5S shows that the structures of guanosine, C8-methylguanosine, and C8-bromoguanosine are predicted to be very similar to one another; however, there are some moderate differences for the C8–N7, C8–N9, and N9–C13 bond lengths. The C8–N9 bond becomes weaker in both the C8-bromoguanosine (1.4028 Å) and C8-methylguanosine (1.4074 Å) predicted structures compared to guanosine (1.3959 Å). The C8–N7 bond becomes stronger in C8-bromoguanosine (1.3111 Å) compared to guanosine (1.3187 Å) but weaker in the C8-methylguanosine (1.3239 Å). The N9–C13 bond becomes weaker in C8-bromoguanosine and has a bond length of 1.4704 Å, which is about 0.0106 Å longer than the bond lengths of those in guanosine and C8-methylguanosine

(1.4598 and 1.4597 Å), and this appears to correlate with the chemical reactivity with the 2-fluorenylnitrenium ion, where the reactions with guanosine and C8-methylguanosine are essentially the same but the reaction with C8-bromoguanosine is noticeably slower. The modest changes in the N9–C13 bond length and possibly the pattern of changes in the bond lengths of the C8–N7 and C8–N9 bonds may be factors influencing the chemical reactivity of the 2-fluorenylnitrenium ion toward the guanosine, C8-methylguanosine and C8-bromoguanosine molecules.

With ns-TR<sup>3</sup> experiments, we observed the fast reaction of the 2-fluorenylnitrenium ion with guanosine, C8-methylguanosine, and C8-bromoguanosine to produce their respective C8 intermediate, C8-methyl intermediate, and C8-bromo intermediate species. It is necessary to point out that in these three C8 intermediate structures, the C8 moiety of the original substrate (H atom or methyl group or bromine atom) still attached to the C8 position in the C8 intermediate species. This is strongly supported by the results that the TR<sup>3</sup> spectra of these three C8 intermediate are similar but not identical, especially the Raman band at  $\sim 1614\text{ cm}^{-1}$  of C8-bromo intermediate being broader than those of C8 intermediate and C8-methyl intermediate, which agrees very well with the DFT-calculated vibrational frequencies of these three structures. The observation of these three C8 intermediates is consistent with the reaction Scheme 1 of Novak and co-workers<sup>39</sup> that proposed the formation of a C8 intermediate cation species that then forms the C8 adduct. Our results are also constituent with the results of McClelland and co-workers that observed formation of C8 intermediates for reactions of a number of arylnitrenium ions with guanine derivatives using time-resolved absorption experiments.<sup>31,32,39</sup> In addition, our TR<sup>3</sup> results are consistent with results of Humphries and co-workers<sup>10</sup> that demonstrated that the CH<sub>3</sub> group is still attached to the final product, which is also consistent with the results of Novak and co-workers<sup>39</sup> that the deprotonation of the H atom at the C8 position is not necessary for the formation of the C8 adducts to take place. Our results do differ from the sequence of events suggested by Humphries and co-workers<sup>10</sup> (on the basis of the limited data available at that time) for the formation of the C8 adduct from the reaction of the arylnitrenium ion with C8-bromoguanosine shown in Scheme 2 in which the bromine atom is not present in the cation intermediate species. Our results indicate that the 2-fluorenylnitrenium ion reaction with C8-bromoguanosine leads to a C8-bromo intermediate species in which the bromine atom is still attached to the C8 position just as in the analogous reactions of the 2-fluorenylnitrenium ion with guanosine and C8-methylguanosine to produce their respective C8 intermediate species. Our TR<sup>3</sup> results that directly observe the reaction in conjunction with the observation by Humphries and co-workers<sup>10</sup> that the C8 adduct **8** is produced from the reaction of an arylnitrenium ion with C8-bromoguanosine indicate that the dehalogenation step occurs after formation of the C8-bromo intermediate species. Since this reaction takes place in aqueous environments, this dehalogenation reaction step may occur via a water-assisted dehalogenation mechanism similar to those found for the dehalogenation of isopolyhalomethanes, halogenated methanols, and halogenated formaldehydes in aqueous solutions.<sup>45</sup>

It is important to note that our present results do not tell us where the initial position of the attack of the 2-fluorenylnitrenium ion occurs on the guanine derivative to form the C8 intermediate species. For example, we cannot distinguish the possibility of initial attack at the N7 position of the guanine derivative followed by fast conversion to the C8 intermediate species versus a mechanism of initial attack at the C8 position

of the guanine derivative to form the C8 intermediate species directly. However, we do observe that the reaction of the 2-fluorenylnitrenium ion with the guanosine, C8-methylguanosine, and C8-bromoguanosine substrates produce their respective C8 intermediates very fast and this formation is correlated with the decay of the 2-fluorenylnitrenium ion signal, which does place lower limits on the rates of any processes that might occur between the generation of the 2-fluorenylnitrenium ion and the formation of the C8 intermediate.

## Conclusions

A nanosecond time-resolved resonance Raman (ns-TR<sup>3</sup>) spectroscopic investigation of the reaction of the 2-fluorenylnitrenium ion with guanosine, C8-methylguanosine, and C8-bromoguanosine was presented. The TR<sup>3</sup> spectra showed that the 2-fluorenylnitrenium ion reacts with guanosine, C8-methylguanosine, and C8-bromoguanosine to form their respective C8 intermediate, C8-methyl intermediate, and C8-bromo intermediate species with the C8 moiety of the original substrate (H atom or methyl group or bromine atom) still attached to the C8 position in the C8 intermediate species. This is consistent with previously suggested reaction mechanisms of Novak and co-workers<sup>39</sup> and McClelland and co-workers<sup>31,32,39</sup> that proposed the formation of a C8 intermediate cation species that then subsequently produces the stable C8 adduct product. The present TR<sup>3</sup> results (that directly examine the reaction as a function of time) in conjunction with the observation by Humphries and co-workers<sup>10</sup> that the C8 adduct **8** is produced from the reaction of an arylnitrenium ion with C8-bromoguanosine indicate that the dehalogenation step occurs after formation of the C8-bromo intermediate species. The C8-bromoguanosine molecule was observed to have a lower chemical reactivity toward the 2-fluorenylnitrenium ion than the guanosine and C8-methylguanosine molecules. The experimental ns-TR<sup>3</sup> spectra of the three C8 intermediates are similar to one another, and this is consistent the results of DFT calculations that found bromine and methyl group substitutions at the C8 position of the C8 intermediate species only have modest perturbations on the overall structure and properties. The DFT calculations indicate that substitution of a methyl group or a bromine atom at the C8 site of guanosine in the C8 intermediates results in perturbation of the character of the C–C aromatic stretch vibrational modes with more C–N stretch motions becoming mixed with the C–C stretch motions and that this in turn results in a modest amount of downshift in the frequency of this Raman feature in the TR<sup>3</sup> spectra of the C8-methyl intermediate and the C8-bromo intermediate relative to the C8 intermediate as well as to noticeable additional broadening of this Raman feature in the C8-bromo intermediate TR<sup>3</sup> spectra.

**Acknowledgment.** This work was supported by grants from the Research Grants Council (RGC) of Hong Kong (HKU 7040/06P to D.L.P. and HKU 7045/06P to P.H.T.). D.L.P. thanks the Croucher Foundation for the award of a Croucher Foundation Senior Research Fellowship (2006–2007) and the University of Hong Kong for an Outstanding Researcher Award (2006).

**Supporting Information Available:** Descriptions of the preparation and characterization of the 2-fluorenyl azide precursor and the C8-methylguanosine sample used in the TR<sup>3</sup> experiments, overviews of the ns-TR<sup>3</sup> spectra with more time delays and wider wavenumber range obtained after photolysis of 2-fluorenyl azide in the presence of guanosine, C8-methylguanosine, and C8-bromoguanosine, comparison of the 10 ns

spectra shown in Figures 1–3 of the paper to the TR<sup>3</sup> spectrum of the 2-fluorenylnitrenium ion reported in ref 36a, comparison of the 15 μs spectrum of Figure 1 with the 8 μs spectrum obtained in ref 38 for the C8 intermediate species, selected structural parameters for the BPW91/cc-PVDZ optimized geometries for the C8 intermediate, the C8-methyl intermediate, and the C8-bromo intermediate species, comparison of the experimental Raman band vibrational frequencies from the ns-TR<sup>3</sup> spectra of Figure 7 to the BPW91/cc-PVDZ calculated normal Raman vibrational frequencies for the C8 intermediate, the C8-methyl intermediate, and the C8-bromo intermediate species, schematic diagrams for the structures of guanosine, C8-methylguanosine, C8-bromoguanosine, and the 2-fluorenylnitrenium ion determined from BPW91/cc-PVDZ calculations, selected structural parameters determined for guanosine, C8-methylguanosine, and C8-bromoguanosine from the BPW91/cc-PVDZ calculations, and Cartesian coordinates, total energies, and vibrational zero-point energies for the optimized geometry from the BPW91/cc-PVDZ calculations for the C8 intermediate, the C8-methyl intermediate, the C8-bromo intermediate, guanosine, C8-methylguanosine, C8-bromoguanosine, and the 2-fluorenylnitrenium ion. This material is available free of charge via the Internet at <http://pubs.acs.org>.

## References and Notes

- Miller, J. A. *Cancer Res.* **1970**, *20*, 559–576.
- Scribner, J. D.; Naimy, N. K. *Cancer Res.* **1975**, *35*, 1416–1421.
- Miller, E. C. *Cancer Res.* **1978**, *38*, 1479–1496.
- Miller, E. C.; Miller, J. A. *Cancer* **1981**, *47*, 2327–2345.
- Singer, B.; Kusmierk, J. T. *Annu. Rev. Biochem.* **1982**, *51*, 655–693.
- Miller, J. A.; Miller, E. C. *Environ. Health Perspect.* **1983**, *49*, 3–12.
- Garner, R. C.; Martin, C. N.; Clayson, D. B. In *Chemical Carcinogens*, 2nd ed.; Searle, C. E., Ed.; ACS Monograph 182; American Chemical Society: Washington, DC, 1984; Vol. 1, pp 175–276.
- Famulok, M.; Boche, G. *Angew. Chem., Int. Ed. Engl.* **1989**, *28*, 468–469.
- Meier, C.; Boche, G. *Tetrahedron Lett.* **1990**, *31*, 1693–1696.
- Humphreys, W. G.; Kadlubar, K. K.; Guengerich, F. P. *Proc. Natl. Acad. Sci. U.S.A.* **1992**, *89*, 8278–8282.
- Kadlubar, F. F. In *DNA Adducts of Carcinogenic Amines*; Hemminki, K., Dipple, A., Shuker, D. E. G., Kadlubar, K. K., Segerbäch, D., Bartsch, H., Eds.; Oxford University Press: Oxford, U.K., 1994; pp 199–216.
- Dipple, A. *Carcinogenesis* **1995**, *16*, 437–441.
- Novak, M.; Kahley, M. J.; Lin, J.; Kennedy, S. A.; James, T. G. *J. Org. Chem.* **1995**, *60*, 8294–8304.
- Cramer, C. J.; Falvey, D. E. *Tetrahedron Lett.* **1997**, *38*, 1515–1518.
- Novak, M.; Kennedy, S. A. *J. Am. Chem. Soc.* **1995**, *117*, 574–575.
- Hoffman, G. R.; Fuchs, R. P. P. *Chem. Res. Toxicol.* **1997**, *10*, 347–359.
- Novak, M.; Kennedy, S. A. *J. Phys. Org. Chem.* **1998**, *11*, 71–76.
- Novak, M.; VandeWater, A. J.; Brown, A. J.; Sanzebacher, S. A.; Hunt, L. A.; Kolb, B. A.; Brooks, M. E. *J. Org. Chem.* **1999**, *64*, 6023–6031.
- Anderson, G. B.; Falvey, D. E. *J. Am. Chem. Soc.* **1993**, *115*, 9870–9871.
- Davidse, P. A.; Kahley, M. J.; McClelland, R. A.; Novak, M. J. *Am. Chem. Soc.* **1994**, *116*, 4513–4514.
- McClelland, R. A.; Davidse, P. A.; Haczialic, G. *J. Am. Chem. Soc.* **1995**, *117*, 4173–4174.
- Robbins, R. J.; Yang, L. L.-N.; Anderson, G. B.; Falvey, D. E. *J. Am. Chem. Soc.* **1995**, *117*, 6544–6552.
- Srivastava, S.; Falvey, D. E. *J. Am. Chem. Soc.* **1995**, *117*, 10186–10193.
- McClelland, R. A.; Kahley, M. J.; Davidse, P. A. *J. Phys. Org. Chem.* **1996**, *9*, 355–360.
- McClelland, R. A.; Kahley, M. J.; Davidse, P. A.; Hadzialic, G. *J. Am. Chem. Soc.* **1996**, *118*, 4794–4803.
- Robbins, R. J.; Laman, D. M.; Falvey, D. E. *J. Am. Chem. Soc.* **1996**, *118*, 8127–8135.
- Moran, R. J.; Falvey, D. E. *J. Am. Chem. Soc.* **1996**, *118*, 8965–8966.
- Michalak, J.; Zhai, H. B.; Platz, M. S. *J. Phys. Chem.* **1996**, *100*, 14028–14036.
- Moran, R. J.; Falvey, D. E. *J. Am. Chem. Soc.* **1996**, *118*, 8965–8966.
- (a) Srivastava, S.; Toscano, J. P.; Moran, R. J.; Falvey, D. E. *J. Am. Chem. Soc.* **1997**, *119*, 11552–11553. (b) Toscano, J. P. *Adv. Photochem.* **2001**, *26*, 41–91. (c) Toscano, J. P. In *Reviews of Reactive Intermediate Chemistry*; Platz, M. S., Moss, R. A., Jones, M., Jr., Eds.; John Wiley and Sons, Inc.: Hoboken, NJ, 2007; pp 183–206.
- McClelland, R. A.; Ahmad, A.; Dicks, A. P.; Licence, V. *J. Am. Chem. Soc.* **1999**, *121*, 3303–3310.
- (a) Sukhai, P.; McClelland, R. A. *J. Chem. Soc., Perkin Trans. 2* **1996**, 1529–1530. (b) Ramillal, P.; McClelland, R. A. *J. Chem. Soc., Perkin Trans. 2* **1999**, 225–232.
- (a) Piech, K.; Bally, T.; Sikora, A.; Marcinek, A. *J. Am. Chem. Soc.* **2007**, *129*, 3211–3217. (b) Wang, J.; Burdzinski, G.; Zhu, Z.; Platz, M. S.; Carra, C.; Bally, T. *J. Am. Chem. Soc.* **2007**, *129*, 8380–8388.
- Kwok, W. M.; Chan, P. Y.; Phillips, D. L. *J. Phys. Chem. B* **2004**, *108*, 19068–19075.
- Srivastava, S.; Ruane, P. H.; Toscano, J. P.; Sullivan, M. B.; Cramer, C. J.; Chiapperrino, D.; Reed, E. C.; Falvey, D. E. *J. Am. Chem. Soc.* **2000**, *122*, 8271–8278.
- (a) Zhu, P.; Ong, S. Y.; Chan, P. Y.; Leung, K. H.; Phillips, D. L. *J. Am. Chem. Soc.* **2001**, *123*, 2645–2649. (b) Zhu, P.; Ong, S. Y.; Chan, P. Y.; Poon, Y. F.; Leung, K. H.; Phillips, D. L. *Chem.—Eur. J.* **2001**, *7*, 4928–4936.
- (a) Chan, P. Y.; Ong, S. Y.; Zhu, P.; Leung, K. H.; Phillips, D. L. *J. Org. Chem.* **2003**, *68*, 5265–5273. (b) Chan, P. Y.; Ong, S. Y.; Zhu, P.; Zhao, C.; Phillips, D. L. *J. Phys. Chem. A* **2003**, *107*, 8067–8074. (c) Chan, P. Y.; Zhu, P.; Phillips, D. L. *Res. Chem. Intermed.* **2005**, *31*, 73–84. (d) Xue, J.; Guo, Z.; Chan, P. Y.; Chu, L. M.; But, T. Y. S.; Phillips, D. L. *J. Phys. Chem. A* **2007**, *111*, 1441–1451.
- Chan, P. Y.; Kwok, W. M.; Lam, S. K.; Chiu, P.; Phillips, D. L. *J. Am. Chem. Soc.* **2005**, *127*, 8246–8247.
- Kennedy, S. A.; Novak, M.; Kolb, B. A. *J. Am. Chem. Soc.* **1997**, *119*, 7654–7664.
- (a) Brown, B. R.; Yielding, L. W.; White, W. E., Jr. *Mutat. Res.* **1980**, *70*, 17. (b) White, W. E., Jr.; Yielding, L. W. In *Wilchek, M., Eds.; Methods in Enzymology Vol. XLVI; Jakoby, W. B., Eds.; Academic Press, Inc.: Orlando, FL, 1977; pp 646–647.*
- Maeda, M.; Nushi, K.; Kawazoe, Y. *Tetrahedron* **1974**, *30*, 2677–2682.
- (a) Frisch, M. J.; Trucks, G. W.; Schlegel, H. B.; Scuseria, G. E.; Robb, M. A.; Cheeseman, J. R.; Zakrzewski, V. G.; Montgomery, J. A., Jr.; Stratmann, R. E.; Burant, J. C.; Dapprich, S.; Millam, J. M.; Daniels, A. D.; Kudin, K. N.; Strain, M. C.; Farkas, O.; Tomasi, J.; Barone, V.; Cossi, M.; Cammi, R.; Mennucci, B.; Pomelli, C.; Adamo, C.; Clifford, S.; Ochterski, J.; Petersson, G. A.; Ayala, P. Y.; Cui, Q.; Morokuma, K.; Malick, D. K.; Rabuck, A. D.; Raghavachari, K.; Foresman, J. B.; Cioslowski, J.; Ortiz, J. V.; Baboul, A. G.; Stefanov, B. B.; Liu, G.; Liashenko, A.; Piskorz, P.; Komaromi, I.; Gomperts, R.; Martin, R. L.; Fox, D. J.; Keith, T.; Al-Laham, M. A.; Peng, C. Y.; Nanayakkara, A.; Gonzalez, C.; Challacombe, M.; Gill, P. M. W.; Johnson, B.; Chen, W.; Wong, M. W.; Andres, J. L.; Gonzalez, C.; Head-Gordon, M.; Replogle, E. S.; Pople, J. A. *Gaussian 98*, revision A.7, *Gaussian 03*, revision B.05; Gaussian Inc.: Pittsburgh, PA, 1998, 2003.
- (a) Kriek, E.; Miller, J. A.; Juhl, U.; Miller, E. C. *Biochemistry* **1967**, *6*, 177–182. (b) Kriek, E. *Chem.-Biol. Interact.* **1969**, *1*, 3–17. (c) Kriek, E. *Chem.-Biol. Interact.* **1971**, *3*, 19–28. (d) Nelson, J. H.; Grunberger, D.; Cantor, C. R.; Weinstein, I. B. *J. Mol. Biol.* **1971**, *62*, 331–346. (e) Fuchs, R. P. P. *Anal. Biochem.* **1978**, *91*, 663–673. (f) Meerman, J. H. N.; Beland, F. A.; Mulder, G. J. *Carcinogenesis* **1981**, *2*, 413–416. (g) Beland, F. A.; Dooley, K. L.; Jackson, C. D. *Cancer Res.* **1982**, *42*, 1348–1354. (h) Evans, F. E.; Miller, D. W.; Levine, R. A. *J. Am. Chem. Soc.* **1984**, *106*, 396–401. (i) Tamura, N.; King, C. M. *Carcinogenesis* **1990**, *11*, 535–540.
- (a) Lee, M.-S.; King, C. M. *Chem.-Biol. Interact.* **1981**, *34*, 239–248. (b) Shapiro, R.; Underwood, G. R.; Zawadzka, H.; Broyde, S.; Hingerty, B. *Biochemistry* **1986**, *25*, 2198–2205. (c) Underwood, G. R.; Price, M. F.; Shapiro, R. *Carcinogenesis* **1988**, *9*, 1817–1821. (d) Van de Poll, M. L. M.; Van der Hulst, D. A. M.; Tates, A. D.; Meerman, J. *Carcinogenesis* **1990**, *11*, 333–339.
- (a) Kwok, W. M.; Zhao, C. Y.; Li, Y.-L.; Guan, X.; Wang, D. Q.; Phillips, D. L. *J. Am. Chem. Soc.* **2004**, *126*, 3119–3131. (b) Zhao, C.; Lin, X.; Kwok, W. M.; Guan, X.; Du, Y.; Wang, D.; Hung, K. F.; Phillips, D. L. *Chem.—Eur. J.* **2005**, *11*, 1093–1108. (c) Lin, X.; Guan, X.; Kwok, W. M.; Zhao, C.; Du, Y.; Li, Y. L.; Phillips, D. L. *J. Phys. Chem. A* **2005**, *109*, 981–998. (d) Phillips, D. L.; Zhao, C.; Wang, D. *J. Phys. Chem. A* **2005**, *109*, 9653–9673.